

Fuzzy PID-Based Method for Controlling Piezoelectric Vehicle Engine Mounts

Hangxu Yang^{1,2,*}, Dongmei Liu^{1,2} and Yongjian Gong¹

¹College of Mechanical and Electrical Engineering, Jinhua Polytechnic, Jinhua 321017, China

²Key Laboratory of Crop Harvesting Equipment Technology of Zhejiang Province, Jinhua 321017, China

Received 3 June 2021; Accepted 11 October 2021

Abstract

Engine mounts are vital vibration dampers for vehicles. Conventionally, such devices adopt passive or semiactive control schemes, which cannot isolate the transmission of engine vibration into vehicles over a wide frequency range. This study proposed a method for actively controlling mounts to improve their vibration isolation characteristics over a wider frequency range. On the basis of analysing the structure and working principle of piezoelectric mounts, the equivalent mechanical and mathematical models were built for the mounts, and fuzzy controllers were designed on the basis of fuzzy proportional–integral–derivative (PID) algorithm. Analysis and simulation were performed on MATLAB, and the accuracy of the control algorithm was verified by experiment. Results show that the dynamic stiffness and damping lag angle, two variables reflecting the vibration isolation characteristics of engine mounts, exhibit consistent variations over a low frequency range (0-30 Hz). Within a high frequency range (30-200 Hz), the changes in dynamic stiffness are approximately consistent, whereas the changes in damping lag angle differ slightly. The engine vibration is attenuated by over 80%. The designed fuzzy PID algorithm is completely applicable to the active control of engine mounts. This study provides a certain reference for the active control design of piezoelectric vehicle engine mounts.

Keywords: Fuzzy PID, Piezoelectric effect, Engine mount, Control method

1. Introduction

Engine mounts (vibration dampers) are installed on vehicle brackets, which are often in a three- or four-point support form. Currently, most of them adopt hydraulic or semiactive control, which has a range of advantages, including isolation of the engine vibration transmission into vehicle frame, effective absorption and attenuation of engine vibration, and good vibration isolation effect [1]. Thus, they have been extensively applied in small family cars. With the ever-heightening requirements on driving comfort, the demand for high-efficiency engine mounts has been growing, and related technical studies have made great progress. Increasing enterprises and institutions have been involved in the development and control system design for engine mounts. Most of them adopt the semiactive control schemes by exploiting the special properties of electrorheological or magnetorheological fluids [2].

With the continuous development of vehicle control algorithms, the semiactive mounts yield undesirable effect in the high frequency range although they can solve the vibration isolation problem in the low frequency range. The semiactive control requires the precision of control scheme on the basis of performance improvement in media, such as electrorheological and magnetorheological fluids, which is technically difficult and brings huge challenges to the study on engine mounts.

Extensive studies have been conducted on the active control engine mounts (e.g., piezoelectric and electrostrictive types) and algorithms [3-4]. Existing active control technologies include the piezoelectric ceramic actuator technology, shape memory metal technology,

electromagnetic actuator technology utilizing smart magnetic materials, and vibration isolation technology exploiting intrinsic characteristics of piezoelectric elements [5-6]. Although the above technologies have been theoretically effective in isolating vibrations based on simulation, problems remain regarding the mount design, the low- and high-frequency vibration isolations, and the efficiency of vibration isolation. Hence, how to improve the isolation efficiency of active engine mounts by accurate mount modeling and appropriate control scheme is an imperative task.

This study conducts equivalent modeling of piezoelectric engine mount and designs fuzzy controllers by using fuzzy proportional–integral–derivative (PID) algorithm. The feasibility of the proposed method is validated through simulation and experiment. The results serve as reference for the development and optimization of piezoelectric active control mounts.

2. State of the art

To date, extensive studies have been conducted on the passive, semiactive, and active engine mounts, and relevant control algorithms. Farag K Omar [7] made a multiobjective optimization design for an orifice-controlled dual-mode semiactive engine mount. This design responds well to the mount dynamic characteristics, especially the stiffness, but is insufficiently effective in the full-frequency vibration isolation. For multiobjective solution of mount parameters, Siano D [8] developed a mathematical model for robust optimization of mount system and optimized the suspension parameters via particle swarm optimization. The experimental results showed that the model had limited

*E-mail address: yanghx_83@126.com

ISSN: 1791-2377 © 2021 School of Science, IHU. All rights reserved.

doi:10.25103/jestr.145.16

effect on the damping lag angle, albeit preferable response to changes in stiffness. Mao Shulin [9] tested the vibration and noise of passive hydraulic mounts over different speed ranges. Although a good vibration isolation effect was achieved in the low-frequency resonance region owing to the use of rubber mainspring material, the vibration isolation effect was poor in the high-frequency and nonresonant regions. Regarding the effects of structural parameters on the mount damping effect, Tian J [10] built a semiactive hydraulic mount model by using fluid-structure coupled finite element method, which was ineffective in terms of dynamic response characteristics and damping attenuation. TAO C. [11] performed dynamic mount modeling and identified relevant parameters by using fractional derivative model. However, he did not explore the vibration isolation characteristics. Concentrating on the identification accuracy of mount model parameters, Chen Shiwei [12] proposed the Bingham model and parameter identification method and explored the restoring force composition of a certain active engine mount. However, the experimental effect of the model was unsatisfactory in the low frequency state. Zheng Ling [13] identified the forward and inverse models of semiactive magnetorheological mounts with Elman neural network. The forward model preferably attenuated the vibration in terms of stiffness and damping adjustment, and the inverse model performs slightly worse regarding the damper size effect on the damping force. Hu Guoliang [14] derived the correlation between damper parameters and damping force by using constitutive mechanical model. Given the directionality of the damper, its installation and setting needed to be considered, and precise manufacturing and machining are required. Although the large volume was found greatly influential to the damping force, the correlation between damping and stiffness was not clearly described. To solve the time lag problem caused by damping, Li Zhihua [15] designed a semiactive mount controller considering time lag. This controller corrected the error of damping force response. However, the response error level was low and cannot reflect the vibration isolation effect of the mount preferably. To explore the effects of mount speed characteristics on the vibration isolation efficiency, Kou Farong [16] developed a semiactive magnetorheological damper and conducted a mechanical analysis, thereby obtaining the speed characteristic curves. However, no mechanical analysis of damper was provided in the high frequency range. Raizada A [17] constructed a dynamic damper model by introducing a neural network algorithm and verified it through experiment. Although the experimental results suggested that the algorithm was feasible, the response to damping changes was lacking. Focusing on the accuracy problem of conventional dynamic mount models, Boada MJL [18] created an inverse dynamic model based on neural network, where the damping force was estimated. However, the vibration response of the model was ineffective in the high frequency range. Peng Zhizhao [19] conducted semiactive control experiments on a test bench by using three different switch control strategies, revealing the superiority of SH-ADD control strategy. However, the three tested strategies still had insufficient control accuracy, especially in controlling the low frequency vibrations, thereby leading to problems, such as poor low-frequency vibration isolation for conventional caterpillar engine mounts. To address the poor modeling and simulation effects of semiactive control for caterpillar vehicle mount systems, Ata WG [20] conducted relevant theoretical study and created a simulation model for such

suspension systems. Despite the good reflection of the semiactive control mechanism, the model was ineffective in attenuating the vibration over the whole frequency range. Miah MS [21] designed a brand-new control scheme, which was used in combination with the unscented Kalman filter observer for observing structural vibrations. Although this scheme well integrated the Kalman filter principle, the dynamic characteristics were not investigated. Bathaei A [22] constructed an 11-degrees of freedom (DOF) model to explore the vibration isolation characteristics of semiactive and magnetorheological dampers. However, he did not explore the response changes in damping lag angle under high frequency conditions. Focusing on the vibration isolation problem of engine mounts in idling state, Oh JS [23] designed a novel sliding mode controller to assess the vibration isolation characteristics of vehicle engines. However, he did not probe the effect of the designed controller on the reduction of vehicle engine vibrations. Pan Gongyu [24] made structural improvement to the original magnetorheological mount by designing a semiactive mount with multiple inertia tracks. He built a 2-DOF model of equivalent stiffness and damping and performed relevant simulations. However, the results suggested that the model had poor effect on dynamic stiffness. To enhance the accuracy of vibration frequency ratio, Aikhuele Daniel O [25] developed a dynamic model comprising surface quality, driving point mechanical impedance, and mount transmissibility. Simulations revealed that the model responded well at low frequencies, whereas it performed poorly at high frequencies. Considering the aging of elastic components, Soltani Payam [26] investigated the effects of mounts and mainspring materials on the dynamic performance. An aging model was created, which preferably reflected the variation trends of dynamic stiffness and damping with engine frequency despite the insufficient attenuation of the force transmitted to the chassis at low frequencies. Fereidooni Amin [27] numerically carried a single-axis parallel active mount, where the least mean square control was adopted to improve the vibration to some extent. However, ineffective improvement was yielded under high-frequency transient conditions.

The above studies focused mainly on investigating the structure, mechanics, modeling, and control strategy of semiactive mounts or passive suspensions and mounts. However, the modeling, algorithms, and strategies for piezoelectric active mounts have been rarely investigated. The study involving the use of fuzzy algorithms in mount control design is rare. Unlike conventional practices, this study designs fuzzy PID controllers through modeling and analyzing the piezoelectric active mount and develops a fuzzy PID algorithm. Relevant simulation and experimentation are conducted, thereby providing reference for the optimization and application of piezoelectric active control mounts.

The reminder of this study is organized as follows. Section 3 designs the piezoelectric mount and build its equivalent mechanical and mathematical models. The fuzzy PID controller is designed, and the experimental scheme is developed. Section 4 performs simulation and experimental analysis to validate the control effect. Section 5 summarizes relevant conclusions.

3. Methodology

3.1 Mechanical and mathematical models

For the studied piezoelectric mount, its 3D model is shown in Fig. 1, and its 2D structure is depicted in Fig. 2.

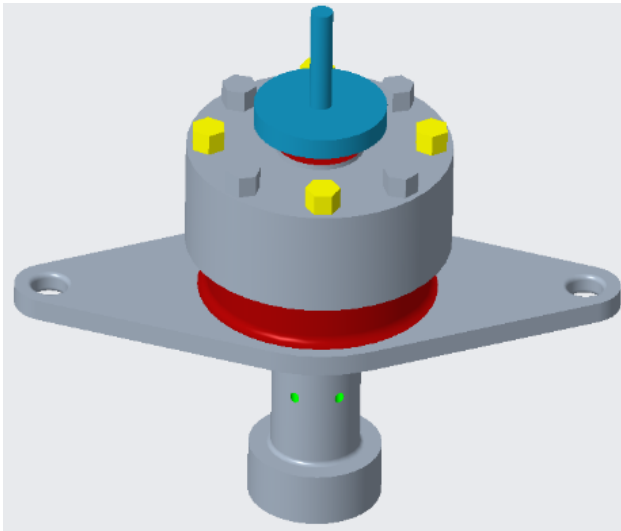
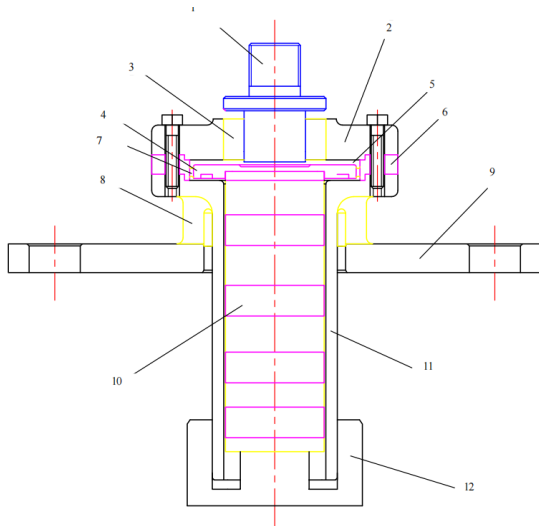


Fig. 1. Three-dimensional model of active mount



1-Small piston,2-Active mount upper cover,3-Connecting rubber,4-Large piston,5-Liquid chamber,6-Intermediate connection,7-Large piston connecting rubber,8-Rubber mainspring,9-Active mount base,10-Piezoelectric actuator,11-Active mount lower casing,12-Actuator base

Fig. 2. Two-dimensional structure of active mount

The thread on the small piston is responsible for connecting to the engine on the vehicle, and base 9 is applied to connect to the vehicle body. When a displacement signal Z is inputted at the upper end of the base, the transmission paths are as follows: The first path starts from the small piston and passes through the intermediate mass, small piston spring, and mainspring rubber to act on the vehicle frame. The second path consists of large piston, liquid chamber, and small piston to form a displacement amplification device. After passing the device, two branches are still found. One branch is acted on the frame by the large piston through the actuator, rubber mainspring, and intermediate mass, and the other branch is acted on the frame by the large piston through the connecting rubber, intermediate mass, and rubber mainspring. During the mechanical modeling of the piezoelectric mount, the following hypotheses are made.

- (1) The effect of change in rubber mainspring temperature on the dynamic characteristics is negligible;
- (2) The liquid is incompressible;
- (3) Considering the insignificant effect of mount on the X- and Y-axis dynamic characteristics, only the Z-axis mechanical and mathematical models are built.

On the basis of the above hypotheses, the mechanical model of the piezoelectric mount is created, as shown in Fig. 3.

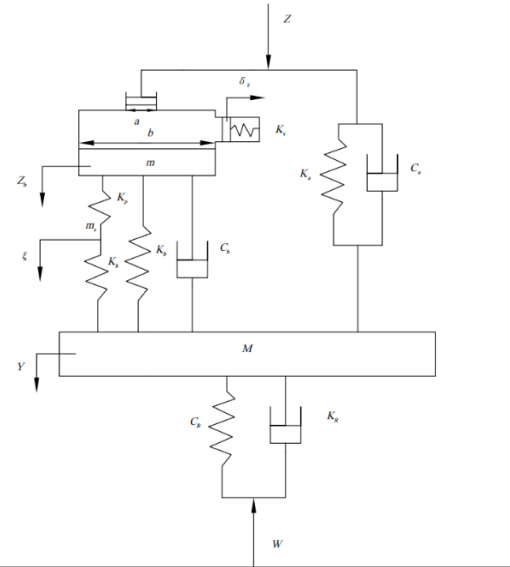


Fig. 3. Mechanical model of the mount

where

- a -Effective area of small piston (mm^2),
 - b -Effective area of large piston (mm^2),
 - K_a - Stiffness of small piston rubber (N/mm),
 - K_b - Stiffness of large piston rubber (N/mm),
 - K_h - Stiffness of piezoelectric actuator bracket (N/mm),
 - K_p - Piezoelectric actuator stiffness (N/mm),
 - K_v - Volume stiffness of liquid chamber (N/mm^5),
 - K_R - Rubber mainspring stiffness (N/mm),
 - C_a - Damping coefficient of small piston rubber (Ns/mm),
 - C_b - Damping coefficient of large piston rubber (Ns/mm),
 - C_R - Damping coefficient of mainspring rubber (Ns/mm),
 - m - Mass of large piston (kg),
 - M - Mass between rubber mainspring and small piston rubber (kg),
 - Z - Forced displacement of small piston (mm),
 - Z_b - Large piston displacement (mm),
 - Y - Intermediate mass displacement (mm),
 - ζ - Piezoelectric actuator displacement (mm),
 - ξ_0 - Maximum amplitude of piezoelectric actuator (mm),
 - W - Force acting on the mount (N).
- Suppose that the potential energy of elastic element is U and the kinetic energy of casing, large piston, and actuator is T , then

$$U = \frac{1}{2}K_a(z-y)^2 + \frac{1}{2}K_v(\delta V)^2 + \frac{1}{2}K_b(z_b-y)^2 + \frac{1}{2}K_t(z_b-y-\xi)^2 + \frac{1}{2}K_R y^2 \quad (1)$$

$$T = \frac{1}{2}mz_b^2 + \frac{1}{2}My^2 + \frac{m_s}{6}(Z_b^2 + y^2 + Z_b y) \quad (2)$$

where K_t denotes the stiffness obtained after connecting the actuator and its support in series:

$$\frac{1}{K_t} = \frac{1}{K_p} + \frac{1}{K_h} \quad (3)$$

The change in liquid chamber volume can be formulated as follows:

$$\delta V = a(z-y) - b(z_b-y) = az - bz_b + (b-a)y \quad (4)$$

Let the viscous damping force acting on the large piston and casing be $Q_1 + Q_2$, then

$$Q_1 = C_b(y - z_b) \quad (5)$$

$$Q_2 = C_a(z - y) + C_b(z_b - y) - C_R y \quad (6)$$

Substituting the above formulas into the Lagrangian equation of motion gives:

$$\frac{d}{dt} \frac{\partial T}{\partial q_j} - \frac{\partial T}{\partial q_j} + \frac{\partial U}{\partial q_j} = Q_j (j=1,2) \quad (7)$$

Let $q_1 = z_b$ and $q_2 = y$, then the following formula can be derived:

$$(m + m_s)z_b + (m_s / 6)y + C_b z_b - C_b y + (K_b + K_t + b^2 K_v)z_b - \{K_b + K_t + b(b-a)K_v\}y = abK_v z + K_t \xi \quad (8)$$

$$(M + m_s / 3)y + (m_s / 6)z_b - C_b z_b - C_a z + (C_a + C_b + C_R)y + \{K_b + K_t + (b-a)^2 K_v + K_a + K_R\}y - \{K_b + K_t + b(b-a)K_v\}z_b = \{K_a - a(b-a)K_v\}z - K_t \xi \quad (9)$$

The above describes the dynamic equations of two piezoelectric mount types. Let

$$\begin{aligned} z_b &= Z_b e^{i\omega t} \\ y &= Y e^{i\omega t} \\ z &= Z e^{i\omega t} \\ \xi &= \Xi e^{i\omega t} \end{aligned} \quad (10)$$

Substituting them into the previous formula yields

$$Y = \frac{N_1 + iN_2}{D} Z + \frac{H}{D} \Xi \quad (11)$$

Where

$$N_1 = [K_a - a(b-a)K_v]F_1 + abK_v F_3 - C_a C_b \omega^2$$

$$N_2 = [C_a N_1 + C_b(K_a + a^2 K_v)]\omega$$

$$F_1 = K_b + K_t + b^2 K_v - (m + m_s / 3)\omega^2$$

$$F_2 = K_b + K_t + (b-a)^2 K_v + K_a + K_R - (M + m_s / 3)\omega^2$$

$$F_3 = K_b + K_t + b(b-a)K_v + m_s / 6\omega^2$$

$$H = K_t(F_3 - F_1) \quad (12)$$

$$D = D_1 + iD_2$$

$$D_1 = F_1 F_2 - F_3^2 - C_h(C_a + C_R)\omega^2$$

$$D_2 = [(C_a + C_b + C_R)F_1 + C_b(F_2 - 2F_3)]\omega \quad (13)$$

After calculating Y , the reaction force $w = C_R y + K_R y$ acting on the mount system can be calculated:

$$W = (K_R + iC_R \omega)Y \quad (14)$$

Suppose that G is the mass of powertrain borne by a piezoelectric mount, then the dynamic force imposed on the engine is

$$F(t) = G \ddot{z} + C \dot{a} + K a z + K_v \delta V \quad (15)$$

The dynamic force transmitted from the mount to the frame is

$$F_T(t) = C_R y + K_R y + G \quad (16)$$

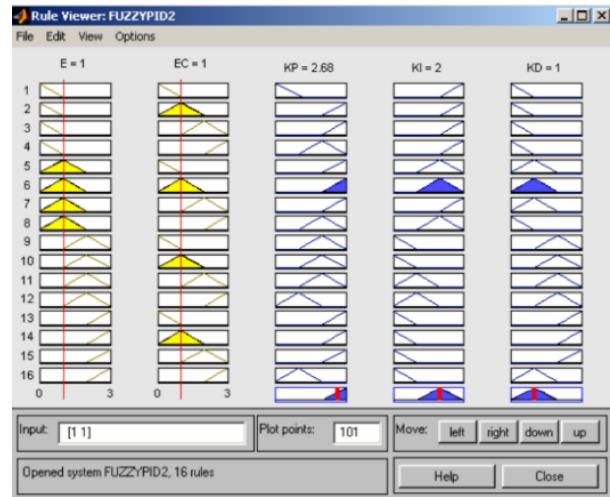
The above equation describes the mathematical model of piezoelectric mount, which is the basis for simulating the mount dynamic characteristics.

3.2 Design of fuzzy PID controller

Conventional PID control features simple principle, ease of use, and strong robustness. It can be used even if the mathematical model of controlled object is inaccurate. Thus, conventional PID control has been widely used in industrial process control for a long time, achieving good control effects. However, in case of changes in the external circumstances, the PID parameters cannot adapt to different working conditions because the conventional PID algorithm is integrated under a particular condition, thereby failing to meet the design performance standards. During the control process, some object parameters are slowly changing or unknown, and some objects are randomly interfered or delayed, which are the so-called uncertainties.

Confronting the above situation, the conventional PID control cannot independently tune the parameters KD, K1, and KP online. Online self-tuning of PID parameters is required to improve the performance of PID controller. In this study, fuzzy PID controller is designed primarily by using the Simulink module of MATLAB, which is a software package used to model, simulate, and analyze dynamic systems. In addition to supporting continuous,

discrete, and hybrid nonlinear/linear systems, it supports multiple rate systems. The features of Simulink are as follows: Simulation and connection functions; modeling with block diagrams; hierarchical modeling architecture; convenient simulation; rich sub model library; supporting multiple control modules from discrete to continuous; providing multiple simulation signal sources; diverse simulation methods, allowing dynamic characteristics analysis of control systems. Aided by this module, the required model of control system is drawn in the Model window, and then system simulation is performed directly by using the functions provided by it. This study designs the fuzzy PID control algorithm via the Fuzzy Logic Toolbox of MATLAB. In accordance with the intrinsic vibration isolation needs of the active mount, a two-input three-output fuzzy inference system is built (Fig. 4). The membership function is defined, as shown in Fig. 5, and the control rules of the inference system are formulated, as shown in Fig. 6.



(a)

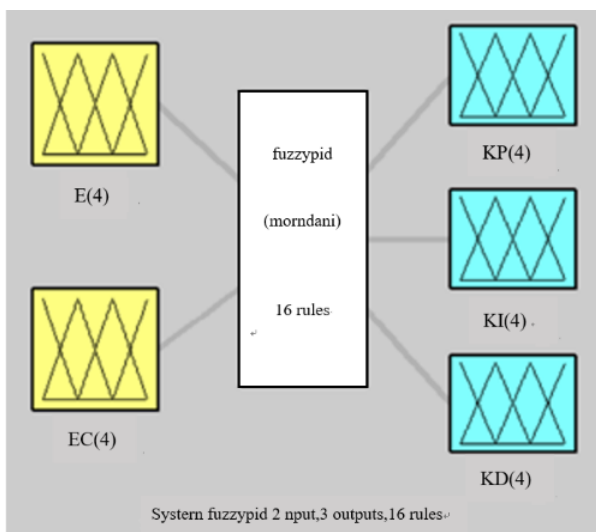


Fig. 4. Mechanical model of the mount

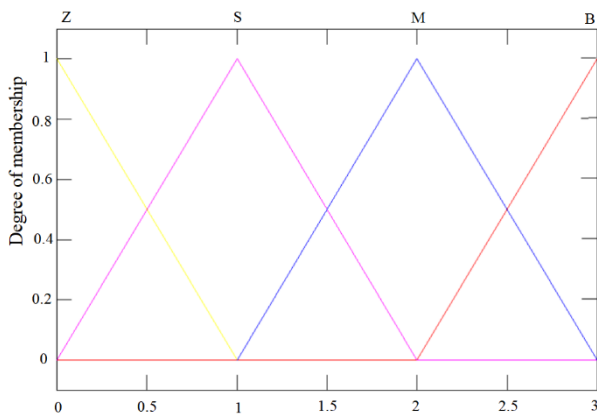
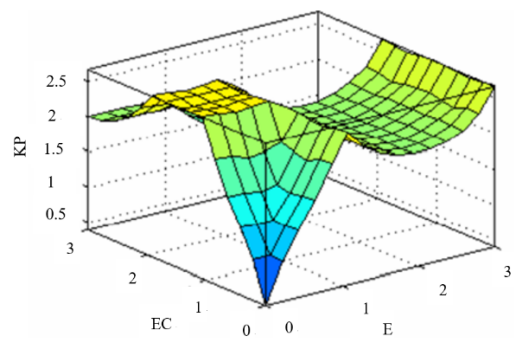


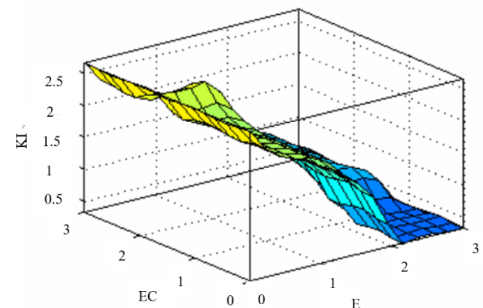
Fig. 5. Membership function

As shown in Fig. 6(a), when the system rate of error change $|ec|$ and system error $|e|$ are quantized as 1, the K_D , K_I , and K_P outputs are 1, 2, and 2.68, respectively. Figs. (b)–(d) depict the K_D , K_I , and K_P outputs on the interval (0, 3).

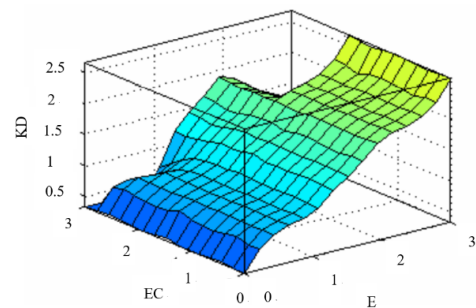
The PID control is integrated into the fuzzy controller to obtain the fuzzy PID controller, as shown in Fig. 7.



(b)



(c)



(d)

Fig. 6. Outputs of fuzzy control system

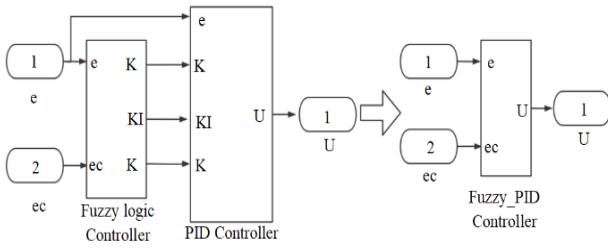


Fig. 7. Fuzzy PID controller

3.3 Experimental design

As shown in Fig.8, the entire experimental facility comprises a test bench and a control device.

(1) Test bench: An active hydraulic mount is installed and fixed on the bench for measuring its dynamic stiffness and lag angle.

(2) Control device: Active control is implemented by utilizing the piezoelectric effect.

During the experiment, the fluid motion in the mount is controlled by the negative pressure vacuum pump. The pressure gauge and adjustable switch are connected in series between the vacuum pump and the intake tube, and the intake pressure of active mount can be adjusted at any time. The assembled facility needs to be placed at 20 ± 3 °C for longer than 18 h to ensure the experimental accuracy.

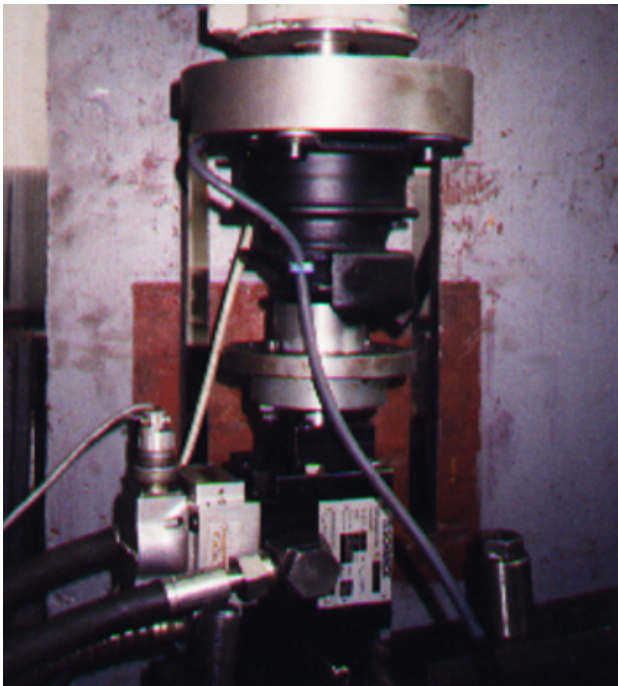


Fig. 8. Experimental setup of active mount

4 Result Analysis and Discussion

On the basis of the built model, the input amplitude of the active mount is considered to be approximately 0.1 mm because the disturbance for engine mounts is millimeter-level under idling conditions. Simulation is performed with $z = \sin(10t)$ and $z = 0.1\sin(100t)$ as inputs. Figs. 9 and 10 illustrate the results.

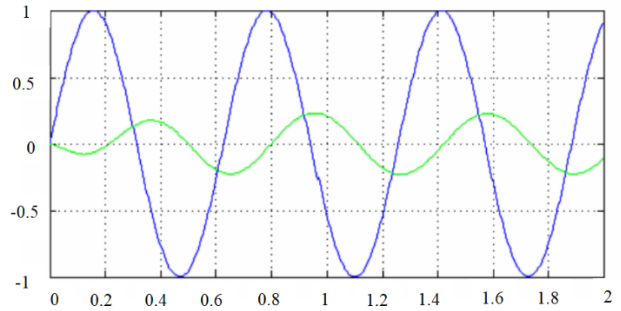


Fig. 9. Response to $z = \sin(10t)$ input

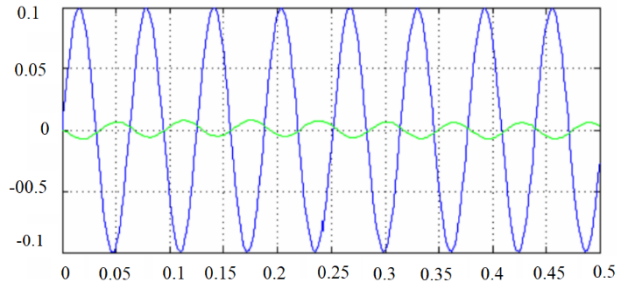
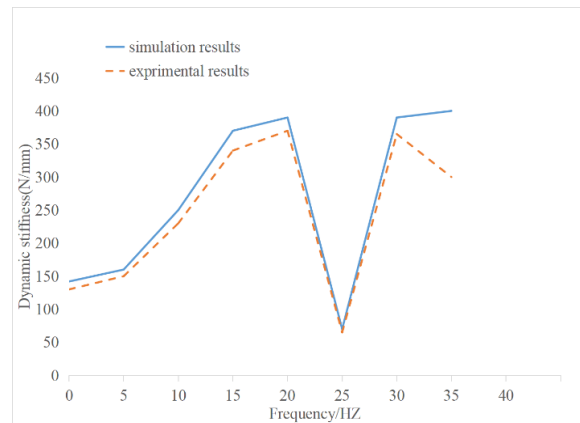
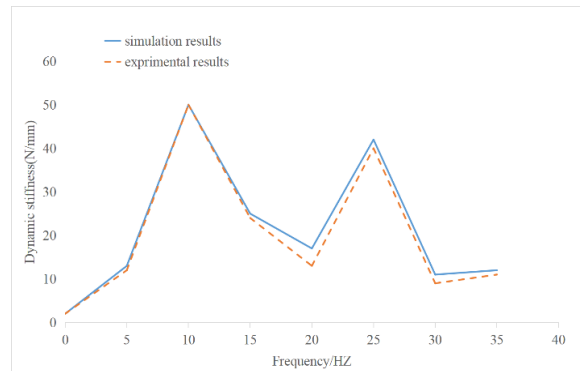


Fig. 10. Response to $z = 0.1\sin(100t)$ input

As shown in the simulation results, the fuzzy PID control model can attenuate the vibrations to over 80%, showing a good effect. The dynamic characteristics of active mount calculated in Matlab/Simulink are compared with the experimental data, and Figs. 11–12 display the results.

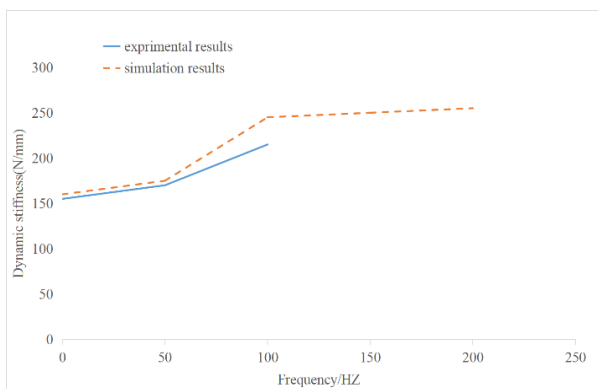


(a) Stiffness comparison

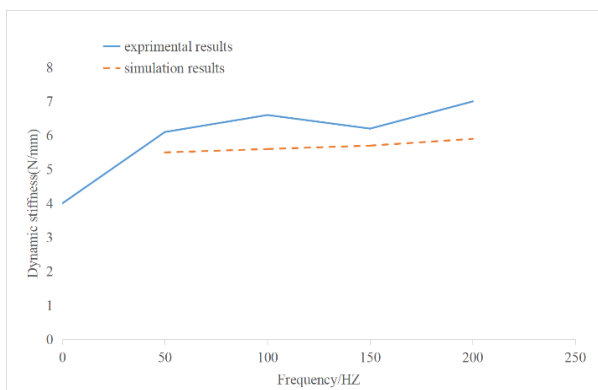


(b) Damping lag angle comparison

Fig. 11. Simulation vs. experimental curves in low frequency range (0-30 Hz)



(a) Stiffness comparison



(b) Damping lag angle comparison

Fig. 12. Simulation vs. experimental curves in high frequency range (30–200 Hz)

The comparison curves in Figs. 11 and 12 show that in the low frequency range (0-30 Hz), the simulated and experimental changes in dynamic stiffness of active mount are highly consistent, with mostly identical parameter values. The damping lag angle exhibits the same variation trend. In the high frequency range (30-200 Hz), the simulated and experimental dynamic stiffness values of the active mount are close, and the numerical variation of the damping lag angle exhibits a slightly differing trend. Simulation and experimental analysis show that the changes in stiffness and damping lag angle at low frequencies differ slightly from those at high frequencies, with each reflecting different variation characteristics. Specifically,

(1) At a low frequency (0-15 Hz) stage, the dynamic stiffness increases gradually with the increasing frequency. This condition is primarily attributed to the flexible control at this stage (generally in the engine starting phase), and the relatively small external interference.

(2) At a low frequency (15-30 Hz) stage, the dynamic stiffness undergoes a rebounding from the bottom (bottom frequency: approximately 22 Hz) with the increase in frequency, during which the tested piezoelectric element is at the endurance fatigue limit. After this stage, the stiffness value is close to 300 N/mm again.

(3) At a low frequency (15-30 Hz) stage, the overall variation trend of damping lag angle differs slightly from

that of dynamic stiffness, exhibiting two peaks near 10 and 23 Hz.

(4) Simulation and experimental comparison reveal that within the high frequency range (30-200 Hz) of active mount control, the stiffness and damping lag angle tend to increase linearly or approximately linearly overall, reaching maximums at around 200 Hz. The stiffness and damping values are relatively less affected by the external environment because the frequency at this point is close to the moderate load condition of vehicles or engines. However, the damping lag angle exhibits a broken-line variation on the basis of the experiment. Specifically, inflection points appear at three frequencies of 70, 120, and 150 Hz, indicating that the damping lag angle is more susceptible to the experimental conditions and external ambient temperature in these several frequency ranges.

5. Conclusions

Starting with the mechanical and mathematical modeling of photoelectric active mount, this study implemented the active mount control by introducing fuzzy PID algorithm, with a view to improving the vibration isolation characteristics of engine mounts and to attenuating the vibrations over a wider frequency range. The variation trends of the mount stiffness and damping lag angle were analyzed in different frequency ranges by combining the simulation and experimental results. The following conclusions were drawn.

(1) In the low frequency range, the stiffness and damping of the active mount fully meet the dynamic characteristic requirements after adopting the fuzzy PID control.

(2) In the high frequency range, the stiffness of the active mount conforms to the dynamic characteristic requirements after adopting the fuzzy PID control.

This fuzzy PID-based study provides a new insight into the vibration isolation study of piezoelectric active mounts. The built mount model is close to reality and offers certain reference for the subsequent exploration of such mount types. The mount model built has certain limitations in investigating the mount dynamic characteristics at high frequencies due to the relatively differing trends of damping lag angle in the high frequency range. Hence, in future study, the present model can be modified by integrating the experimental data of high-frequency vibration attenuation to achieve more accurate and efficient vibration isolation of active mounts over the whole frequency range.

Acknowledgements

This work was supported by the National Key Research and Development Program of China during the 13th Five-Year Plan Period (No. 2016YFD0701003).

This is an Open Access article distributed under the terms of the Creative Commons Attribution License.



References

- Wei, X. K., Zhu, M., "A semi-active control suspension system for railway vehicles with magnetorheological fluid dampers". *Vehicle System Dynamics*, 54(7), 2016, pp.1-22.
- Liu, X. A., Lu, Z. P., "Research on design method of three-cylinder engine mounting system". *Journal of Vibration Engineering*, 29(5), 2016, pp.804-813.

3. Zhang, X. G., JC, Y. S., "Multi objective optimization of automotive engine mounting system". *Mechanical science and technology*, 34(12), 2015, pp.1940-1946.
4. Hu, Q., Chen, J., Sheng, Z. L., "Robust optimal design of an engine mounting system considering isolation rate". *Noise and vibration control*, 35(4), 2015, pp.840-845.
5. Fu, J. H., W, H., Chen, Z. M., "Research on sub target control of electromagnetic active mount system". *Journal of Chongqing University of Technology (NATURAL SCIENCE)*, 34(7), 2020, pp.10-18.
6. Cheng, Z.M., Wang, H., Cheng, Y., "Research on hierarchical control strategy of automotive powertrain active mount system". *Vibration and shock*, 39(15), 2020, pp200-206.
7. Farag, K.O., Mohamed, Y. E. S., "Time and frequency analyses of dual-fuel engine block vibration". *Fuel*, 20(3), 2017, pp.884-893.
8. Siano, D., "Knock detection in SI engines by using the discrete wavelet transform of the engine block vibrational signals". *Energy Procedia*, 18(8), 2015, pp.678-688.
9. Mao, S.L., "Analysis and experimental study on interior noise caused by engine". Master thesis of Shenyang Ligong University, China, 2016, pp.25-29.
10. Tian, J., Jiang X., Liu G., Dynamic characteristics of semi-active hydraulic engine mount based on fluid structure interaction FEA". In: *Proceedings of the 3rd International Conference on Mechanical and Electronics Engineering*, Osaka, Japan: ICMEE, 2018, pp.310-315.
11. Tao, C., Zhu, H., Xu P., "Frequency-dependent hydraulic engine mount with five- par ammeters fractional derivative model in vehicle model". In: *World Congress and Exhibition*, Detroit, United States: SAE, 2019, pp.210-215.
12. Cheng, S. W., D, P. F., "Parametric modeling and identification of magnetorheological engine mount". *Journal of Mechanical Engineering*, 52(8), 2016, pp.29-35.
13. Zheng, L., Dong Z. X., Pang, J., "Vehicle semi-active vibration control based on engine magnetorheological mount". *Automotive Engineering*, 38(2), 2016, pp.221-228.
14. Hu, G. L., Liu Q. J., "Influence of MR damper parameters on vibration reduction effect of vehicle suspension". *Mechanical science and technology*, 37(6), 2018, pp.930-935.
15. Li, Z. H., "Study on characteristics and semi-active control strategy of valve-controlled damper". Master thesis of Jilin University, China, 2017, pp.32-39.
16. Kou, F. R., "Design and test of automotive magnetorheological semi-active suspension system". *Transactions of The Chinese Society of Agricultural Machinery*, 47(4), 2016, pp.280-287.
17. Raizada, Singru P., "Development of an experimental model for a magnetorheological Damper Using artificial Neural networks (Levenberg-Marquardt Algorithm)". *Advances in Acoustics & Vibration*, 20 (2), 2016, pp.1-6.
18. Boada M. J. L., Boada B. L., Diaz V., "A novel inverse dynamic model for a magnetorheological damper based on network inversion". *Journal of Vibration & Control*, 24(15), 2018, pp.3434-3453.
19. Peng, Z. Z., Zhang, J. Q., "Experimental study on magnetorheological semi-active suspension". *Automotive Engineering*, 40 (5), 2018, pp.15-21.
20. Ata, W. G., Salem, A. M., "Semi-active control of tracked vehicle suspension incorporating magnetorheological dampers". *Vehicle System Dynamics*, 53(25), 2017, pp.1-22.
21. Miah, M. S., Chatzi, E. N., Weber, F., "Semi -active control for vibration mitigation of structural systems incorporating uncertainties". *Smart Material Structures*, 24(5),2015, pp.35-38.
22. Bathaei, A., Zahrai, S.M, Ramezani, M., "Semi-active seismic control of an 11-DOF building model with TMD plus MR damper using type-1 and-2 fuzzy algorithms" . *Journal of Vibration and Control*, 24(13), 2018, pp.2938-2953.
23. Oh, J. S., Choi, S. B., "Ride quality control of a full vehicle suspension system featuring magnetorheological dampers with multiple orifice holes" . *Frontiers in Materials*, 28(6),2019, pp.1-10.
24. Pang, G. Y., Wang, Q. Q., Yang, X., "Study on dynamic characteristics and PID control of automotive engine magnetorheological mount". *Electromechanical engineering*, 32(6), 2015, pp.751-753.
25. Aikuele, D., O., "Note on the modelling of the frequency response of an engine mount based on the engine vibration". *The European Journal Plus*, 136(7),2021, pp.83-89.
26. Soltani, P., Wagg, D., Pinna, C., Whear, R., "Dynamic Modelling of a Hydraulic Engine Mount Including the Effects of Elastomer Ageing". *SAE International Journal of Engines*, 14(1),2021, pp.99-114.
27. Fereidooni, A., Craham, C. E., Wickramasinghe V., "Investigation of a Parallel Active Vibration Isolation Mount for Mitigating N/Rev Helicopter Vibrations". *Journal of Dynamic Systems, Measurement, and Control*, 142(7), 2020, pp.112-116.